The Design and Testing of an Electromechanically Actuated Pitot Probe to Characterize Flow in a Mach 7 Wind Tunnel

Ivana Chen[1] and Christopher S. Combs[2]
The University of Texas at San Antonio, San Antonio, Texas, 78249, USA

Vehicles designed for hypersonic speeds are tested in high Mach number wind tunnels to understand the effects of aerothermodynamic phenomena which occur during flight. Boundary layers occurring on hypersonic vehicle airframes are significantly influenced when impinged upon by shock waves. This interaction can lead to flow separation which can cause vehicle stall, structural damage, and inlet unstart. The successful study of boundary layers is heavily reliant on the precise quantification of flow properties. In the hypersonic flow regime, the temperatures generated by the flow are very high and can deform the materials of aircraft, damage their structures, and decrease their performance capabilities, both structurally and aerodynamically. Hypersonic wind tunnels can be employed to experimentally study these effects and improve the design of aircraft and space vehicles to prevent material failures and ensure safety. The need to perform such boundary layer research in the newly constructed UTSA Mach 7 Ludwieg tube wind tunnel facility underscores the significance of developing an accurate and reliable Pitot tube measuring system. Commonly used on aircraft and in wind tunnels, Pitot tubes measure flow speed by placing a tube directly into the flow stream. This project studies the turbulent boundary layer of the test section walls by employing a newly designed and constructed traversing Pitot probe to collect the boundary layer data. In hypersonic flow, a detached bow shock will form when the probe enters the flow stream. This experiment therefore utilizes the Rayleigh Pitot tube relation to calculate the Mach number. Through data from this study the hypersonic air flow properties of the wind tunnel are accurately and reliably characterized by developing velocity profiles using Python scripts which imparts valuable information on the boundary layer region in this facility's Mach 7 flow.

I. Nomenclature

a	=	Speed of sound
M	=	Mach number
P	=	Static pressure
P_0	=	Stagnation pressure
Pr	=	Prandtl number
R	=	Universal gas constant
T	=	Static temperature
T_0	=	Stagnation temperature
U	=	Velocity
δ	=	Boundary layer thickness
γ	=	Specific heat

[1] Undergraduate Research Assistant, Department of Mechanical Engineering, AIAA Student Member.
[2] Dee Howard Assistant Professor, Department of Mechanical Engineering, AIAA Senior Member.

II. Introduction

A wind tunnel is a fundamental device for experimentation and characterization of aerodynamic phenomena. Frank Herbert Wenham and John Browning built the first wind tunnel in 1871 and revolutionized the simulation of airstream behaviors on aircraft and spacecraft models [1]. Engineers designing vehicles for hypersonic speeds utilize high-speed wind tunnels to conduct testing in a relevant flight environment before the first vehicle flight [2]. Wind tunnels are categorized into two main categories: continuous wind tunnels and intermittent wind tunnels. Continuous wind tunnels allow for longer test runs—providing more time to measure flow conditions—but are mostly limited to low air flow speeds because of the power required to maintain the longer flow time. Intermittent tunnels are less costly and simpler than continuous tunnels. High-speed tests usually employ intermittent tunnels because the high power is only needed for a very short run time and allows short turnaround time [3]. Wind tunnels provide many economic, safety, and technical advantages in aviation and flight sciences.

Researchers at the University of Texas at San Antonio (UTSA) have constructed a Mach 7 Ludwieg Tube-based wind tunnel [4]. Mach number is the ratio of the velocity of the fluid to the velocity at which sound travels in the fluid; in aerodynamics, that fluid is typically air. Based on the compressibility effects of air, flight Mach numbers can be grouped into four flight regimes: subsonic (Mach 0 to 0.8), transonic (Mach 0.8 to 1.2), supersonic (Mach 1.2 to 5.0), and hypersonic (Mach 5.0 and above). This study will focus on hypersonic flow regimes where the speed is greater than five times the speed of sound. Though negligible in other flow regimes, an object's effect on the chemical bonds of the fluid cannot be ignored in hypersonic flows, and interactions between shock waves and boundary layers must be considered along with compressible flow effects. In the hypersonic flow regime, the temperatures generated by the flow are very high and can deform the materials of aircraft, damage their structures, and decrease their performance capabilities, both structurally and aerodynamically [5]. Low enthalpy flows in a wind tunnel lack high temperatures meaning testing can occur without a high energy requirement. Hypersonic wind tunnels can be employed to experimentally study these effects and improve the design of aircraft and space vehicles to prevent material failures and ensure safety.

III.Theory and Background

A Pitot probe is a device used for measuring the air's speed in wind tunnels, and was originally invented to measure river water speed by Henri Pitot in 1732 [6]. Commonly used on aircraft and in wind tunnels, Pitot tubes measure flow speed by placing a tube directly into the flow stream. One type is a Pitot-Static tube which has two separate openings. One opening is positioned directly facing the streamline and measures the stagnation pressure of the air. The second port in the pitot tube is positioned perpendicular to the flow and measures the static pressure [7]. Another probe type, known as a Pitot tube, utilizes a tube with only one opening to measure the stagnation pressure and then measure the static pressure from a port perpendicular to the flow that is separate from the Pitot tube. The stagnation and static pressures are used to calculate the velocity of the flow by applying Bernoulli's equation and converting the pressure energy to the kinetic energy. Bernoulli's principle applies to isentropic flow and states that the total energy of pressure, kinetic, and potential energy of a unit volume remains constant as long as it travels along a streamline [8]. In hypersonic flow, a detached bow shock will form when the probe enters the flow stream. This experiment will therefore utilize the Rayleigh Pitot tube relation to calculate the Mach number [9]. With the Mach number, the velocity can then be calculated. The Rayleigh Pitot tube formula is shown below, with γ being the specific heat of the air and P_1 being the static pressure before the detached normal shock:

$$\frac{P_{02}}{P_1} = \left[\frac{(\gamma+1)^2 M^2}{4\gamma M^2 - 2(\gamma-1)}\right]^{\frac{\gamma}{\gamma-1}} \left[\frac{1-\gamma+2\gamma M^2}{\gamma+1}\right]^3 \tag{1}$$

The static temperature profile equation is:

$$T = T_0 * \left(1 + \frac{\gamma-1}{2} M^2\right)^{-1} \tag{2}$$

The speed of sound equation is:

$$a = \sqrt{\gamma R T} \tag{3}$$

The velocity profile equation is:

$$U_e = M * a \tag{4}$$

Boundary layers are viscous layers of fluid that form between the solid surface of an object and the free stream of the fluid. In the boundary layer, the velocity is not constant like the free stream section of the flow [10]. The dimensionless Reynolds number varies greatly in the boundary layer region [11]. The Reynolds number is the ratio of

the inertia force to the viscous force lower value of the Reynolds number signals that the boundary layer is laminar and a higher value indicates an unsteady, or turbulent boundary layer [12].

When a vehicle attains hypersonic flight, the unsteady flow phenomena of shock-wave/boundary-layer interaction (SWBLI) occur. The shock wave interactions can alter the boundary layer and cause flow separation which abruptly increases pressure. These adverse pressure gradients can cause high thermal loads while the flow separation can lead to engine inlet unstarts and flameouts in air breathing propulsion systems [13]. These effects are dangerous and can lead to structural fatigue and failure, among many other airborne performance problems; therefore, understanding of these unique aspects will lead to safer aircraft designs and avoid catastrophic accidents from occurring. These requirements and drivers all point to the significance and necessity of an accurate and reliable Pitot tube to help characterize these boundary layers for tests within the Mach 7 wind tunnel.

The purpose of this project was to study and characterize the turbulent boundary layer of the Mach 7 wind tunnel test section walls. This was achievable by designing a pitot probe that could translate the pressure measurements across the boundary layer of the calculated value of about 50.8 mm (2 in) in height and accurately plot the velocity profiles. The most notable criteria for success of this project were: the opening between the probe and the test section frame shall be securely sealed for the Pitot probe to correctly translate across the entire boundary layer, and the Pitot probe shall be reliable and reusable for future experiments in the Mach 7 wind tunnel.

The first objective was to design and construct a pitot probe to collect data of the boundary layer near the UTSA Mach 7 wind tunnel test section walls. The device would be mounted to a motor to allow vertical translation during testing and be integrated into the test section frame of the wind tunnel. The seal at the frame opening must ensure the tunnel chamber remained airtight and could be drawn to a vacuum.

The second objective of this project was to collect pressure measurements along the boundary layer, which was calculated to have a thickness of less than 50.8 mm (2 in) from preliminary investigations. The collected data was to be converted to the velocity of the flow and display the velocity profiles of the boundary layer within the wind tunnel.

IV. Experimental Methods

A. Wind Tunnel

As previously mentioned in the introduction, this project performed experiments at the Mach 7 Ludwieg Tube wind tunnel at the University of Texas at San Antonio (UTSA). The wind tunnel receives air through a compressor into an 18.29 m (60 ft)-long driver tube where a diaphragm confines the high-pressure gas from entering the test section until the pressure ruptures the diaphragm. The driver tube for the wind tunnel is capable of being pressurized to approximately 13.7 MPa (2,000 psig) [14]. The diaphragm burst forms an expansion wave travelling upstream into the driver tube causing flow to propagate through the nozzle which increases the velocity of the gas to pass through the test section. The dimensions of the test section cross section are 200 mm x 200 mm (8 in x 8 in). With the test gas being air, the pressure ranges from 3.33 to 190 kPa (0.483 to 27.5 psi) and the temperatures 64.8 to 679 K (-343 to 763 °F) in the test section. Figure 1 presents an image taken from the UTSA Hypersonics website of the Ludwieg tube facility this project will use [15].

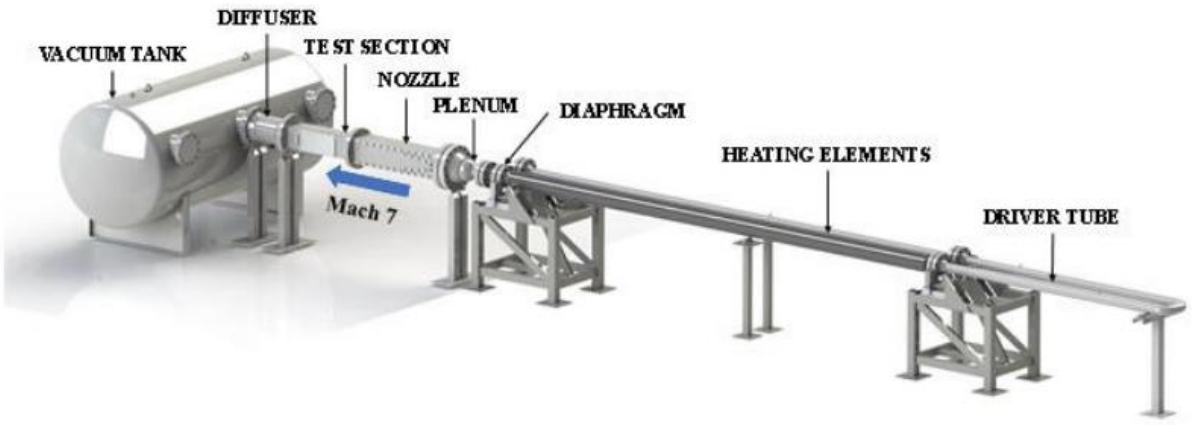

Figure 1. The UTSA Ludwieg tube

B. Ceiling Opening

The ceiling plug attached to the test section floor has a machined opening sealed by a removable plug to allow testing with different instrumentation and models in the wind tunnel. In this experiment, a 15.5 cm by 9.40 cm (6.1 in by 3.7 in) stainless steel plug holds the Pitot probe and is bolted onto the test section. The plug has a wall to mount the actuator in its vertical orientation and a cylindrical opening for the Pitot probe to extend through the plug and into the test section. Only the 2.68 cm (1.06 in) diameter cylinder extends into the inner test section. On the cylinder below the rectangular plug, an O-ring groove houses an AS-568-118 Nitrile 70 O-ring. Vacuum grease improves sealing performance and makes the O-ring easier to install. The surface between the cylinder and the Pitot probe has a 0.4 µm (16 µin) surface finish. The design ensures the plug is flush with the ceiling to avoid creating a step that would adversely affect the air flow.

C. Pitot Probe

The probe is comprised of two 304 stainless steel hypodermic tubing sizes. The inner tube has a 14XX gauge size with a nominal wall thickness of 0.0762 mm (0.003 in) and a 1.96 mm (0.077 in) inner diameter. The 431.8 mm (17 in) long inner tube was placed inside a 13X gauge size tube to be clamped by an aluminum sleeve to the carriage mount of the linear actuator. The Pitot probe employs the aluminum sleeve clamp to allow adjustments in its positioning inside the test section. For this experiment, the starting position of the probe is 50.8 mm (2 in) from the test section wall so that the probe reaches the wall and returns to its original position. Due to the thickness of the 14XX hypodermic tube, the closest distance the probe can measure from the wall is 0.0762 mm (0.003 in).

The outer tube has a 2.16 mm (0.085 in) nominal inner diameter and a wall thickness of 0.127 mm (0.005 in). The length of the outer tube probe is 308.4 mm (12 in.). For measuring the flow, the bottom of the probe has another piece of the 14XX hypodermic tubing silver soldered to the side of the vertical tube. The bottom of the probe uses JB weld to block the bottom opening of the probe.

The opening between the Pitot probe and the ceiling plug is sealed by two AS-568-012 Polyurethane 90 Duro O-rings. The O-ring grooves is fabricated using aluminum and attaches to the outer Pitot tube 251.5 mm (9.9 in) from the bottom of the Pitot probe. Having the surface finish on the groove sides to be 0.8 µm (32 µin) and using O-ring grease helps the probe to move dynamically.

D. Pressure Transducer

The Kulite XCQ-062 pressure transducer is placed inside the inner hypodermic tube to minimize the pressure waves travel distances from the wind tunnel. The transducer has a nominal diameter of 1.68 mm (0.066 in) and has a pressure range of 345 kPa (50 psi.) The transducer is fixed inside the probe with silicone sealant. The pressure measurements are acquired with a Teledyne LeCroy wavesurfer 510.

E. Linear Actuator

This project utilizes the Tolomatic MXB-U 25 Rodless Belt Drive actuator powered by a Nema-34 stepper motor. The stroke length of the linear actuator is 102 mm (4 in) and reaches the peak speed of 1,000 mm/s (39.37 in/s.) The weight of the unit that includes the actuator, motor, and motor mount is 5 kg (11 lb.). The repeatability is 0.051 mm (0.00201 in) and the accuracy is 0.051 mm per 300 mm (0.00201 in per 11.8 in.). The motion positioning is configured with the Tolomatic ACS stepper driver. The driver is connected to a 48V power supply. Figure 2 illustrates the circuit diagram of how the electrical components were wired together.

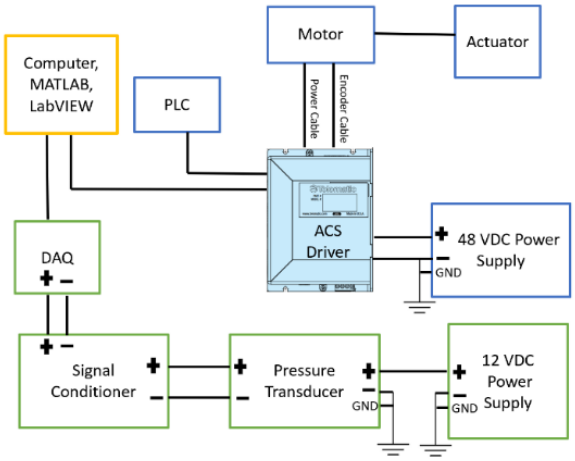

Figure 2. Circuit diagram

Figure 3 exhibits the Pitot probe system consisting of the ceiling plug, actuator, motor, and the probe assembled onto the test section ceiling. The Pitot probe opening inside the test section measured 457 mm (18.0 in) in relation to the test section nozzle exit. Figure 4 shows the physical setup of the system.

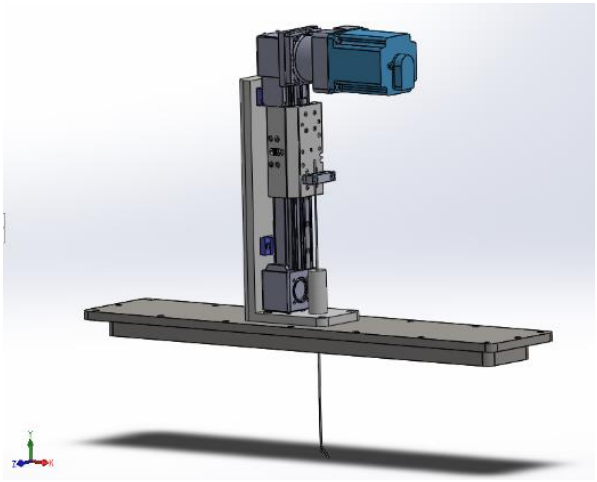

Figure 3. 3D model of the Pitot probe assembly on test section ceiling

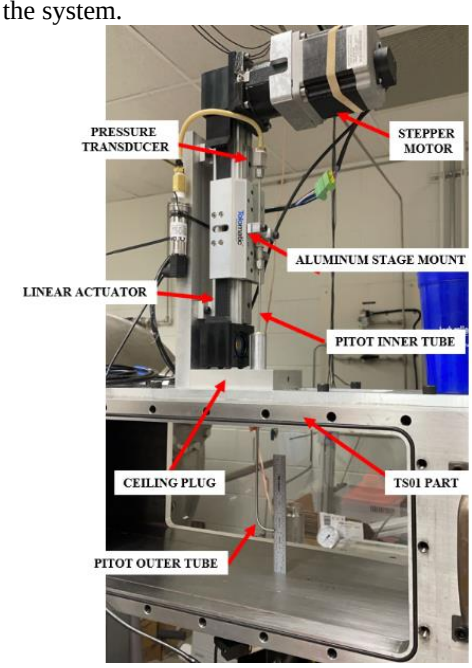

Figure 4. Physical setup of the Pitot probe system

Because the travel distance of the actuator ha a stroke length of 104 mm (4 in) which is less than of the wind tunnel test section height, multiple runs with different starting heights were required to obtain the pressure measurements throughout the entire test section. For each run, a high-speed triggering system initiated the data acquisition, and these points were synchronized using a Stanford Research Systems (SRS DG645) device and exported to a Microsoft Excel file.

The DAQ system acquired the time, probe pressure, plenum pressure, and static pressure. The probe position, Mach number, and velocity values were calculated using a Python code from the values obtained by the DAQ system.

V. Results and Discussion

Five separate runs were required to scan the entire height of the test section and the data acquired were

combined into one for computational analysis. These probe pressure readings for the five runs are shown in Figure 5.

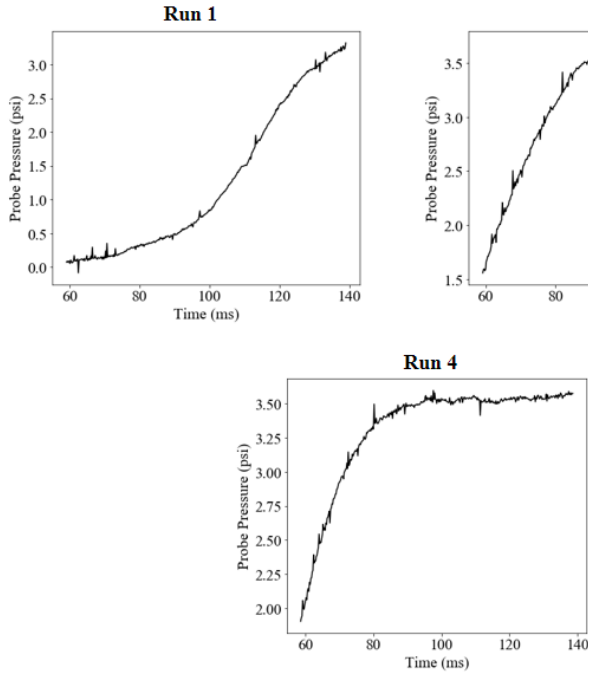

Figure 5. Probe pressure readings for all runs

Knowing the pressure at each cross-section position in the test section, the Mach number could be calculated. The Mach number for each point was calculated using the Rayleigh-Pitot tube formula (Eqn. 1) with P_{02} as the stagnation pressure (psi), P_1 as the static pressure average (psi) multiplied by the P/P_0 ratio value of 1.84×10^{-4} for Mach 7.2 calculated using isentropic flow relations in perfect gas when gamma is 1.4 degrees. The cross-section position versus Mach number plot is shown in Figure 6.

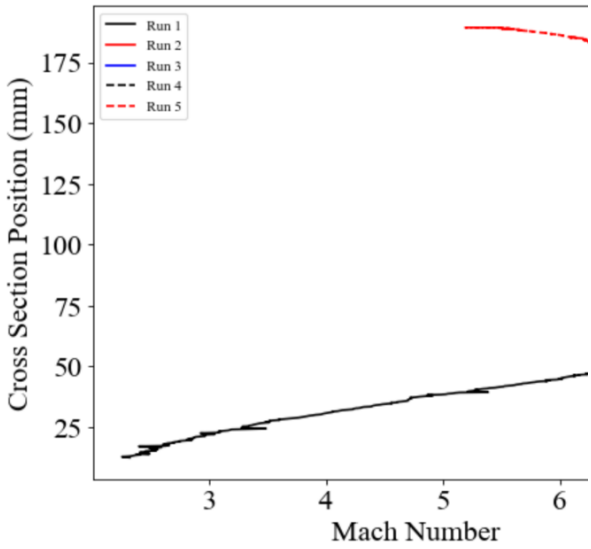

Figure 6. Mach number plot of the wind tunnel test section

With the Mach numbers found for each point, the velocity profile could be calculated. Using 298K for stagnation temperature (T_0), 0.713 for the Prandtl number (Pr), 287 $\frac{J}{kg*K}$ for the universal gas constant, and the recovery factor as $Pr^{1/3}$, the velocity profile was calculated after finding the static temperature and speed of sound profiles.

The velocity profile for the entire test section is presented in Figure 7. The relationship shows that the freestream core has an average velocity of 732 m/s.

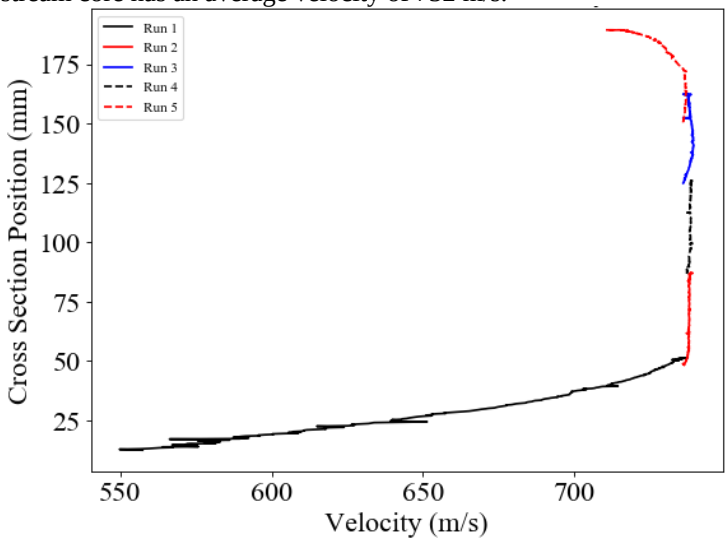

Figure 7. Velocity profile of the wind tunnel test section

Figure 8 and Figure 9 are the velocity profiles for the boundary layers of the test section floor and ceiling by truncating the combined data to the first and second runs for the test section floor and the fifth run for the ceiling. The boundary layer thickness (δ) was calculated using the 95% boundary layer thickness principle which is $u(\delta) = 0.95U_e$. The δ of the test section floor was calculated to be 38.2 mm (1.50 in) and the δ of the test section ceiling was calculated to be 23.6 mm (0.928 in).

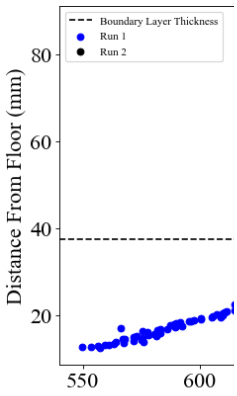

Figure 8. Boundary layer thickness of the test section floor

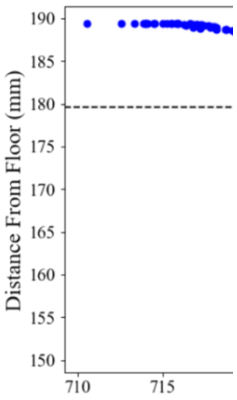

Figure 9. Boundary layer thickness of the test section ceiling

To decrease the gap between the pressure measurement collection and the test section ceiling and floor, a new Pitot probe shape was tested as exhibited in Figure 10 inside the test section. Instead of soldering an inlet to the probe, an inner tube was placed inside the outer tube and bent into a gooseneck shape. With the new shape, the experiment was repeated, and velocity profiles were generated.

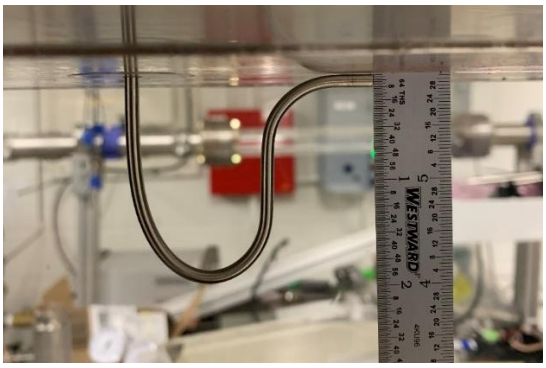

Figure 10. Gooseneck probe shape

Figure 11 is the velocity profile for the boundary layer at the test section ceiling. Figure 12 is the velocity profile for the boundary layer at the test section floor. These plots show that the new Pitot probe shape allowed closer measurement collection to the test section ceiling and floor.

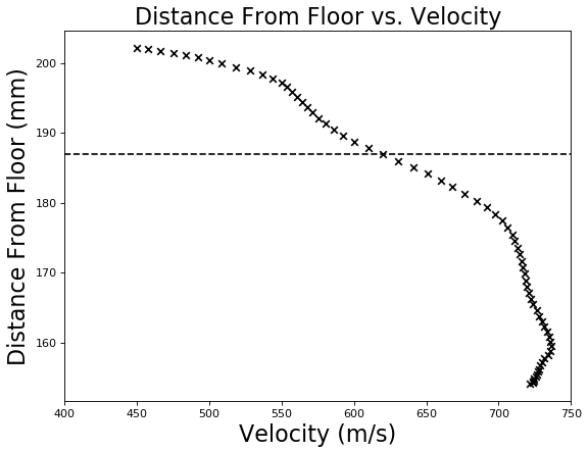

Figure 11. Boundary layer thickness of the test section ceiling from the second experiment

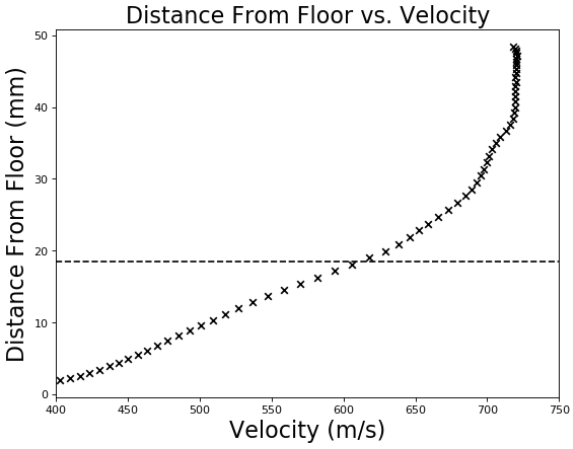

Figure 12. Boundary layer thickness of the test section floor from the second experiment

Ansys Fluent CFD software simulations that had been conducted in previous experiments at the wind tunnel facility provided theoretical values of the Mach number, velocity, and boundary layer thickness [16]. Table 1 compares the experiment findings of the wind tunnel facility from this experiment to the theoretical results obtained from CFD.

Table 1. Comparison of experimental and theoretical results

Data Source	Mach Number	Velocity (m/s)	Boundary Layer Thickness (mm)
Pitot Probe	7.2	732	27 (floor) & 24 (ceiling)
Ansys Fluent Simulations	7.05	736	25

VI. Conclusion

This experiment studied the turbulent boundary layer of the Mach 7 wind tunnel test section walls by designing and constructing a traversing Pitot probe system to collect pressure data of the boundary layer. The Pitot probe setup using a linear actuator and stepper motor allowed the Pitot probe to travel 50.8 mm (2 in) in 80 ms, while the mounting design with the use of dynamic O-rings allowed the test section to seal to a vacuum. Velocity profiles were calculated from the pressure results acquired by the DAQ system. The velocity profiles confirmed that the facility produces a Mach 7.2 flow and that the boundary layer thicknesses can be observed and studied.

The results from this project are useful for future investigations with the Mach 7 wind tunnel facility. The Pitot probe has been proved to be reliable and accurate. It can be used for future experiments for characterizing flow in different working fluids of gases, and the Python code developed in this study can model the velocity profiles in experiments. The system can be applied to other wind tunnels with different speed regimes that requires a traversing mechanism with some instrumentation adjustments for obtaining appropriate measurements. In conclusion, the Pitot probe system design was successful in characterizing the boundary layer region in hypersonic flow.

Acknowledgments

I. Chen thanks Dr. Christopher Combs and Eugene Hoffman for their support and invaluable guidance which have been instrumental in developing and completing this project. I. Chen would like to acknowledge the AFOSR (Award #FA9550-20-1-0190) NASA, the University of Texas at San Antonio VPREDKE awards and the College of Engineering Undergraduate Research Program for funding this project.

References

1. Lee, J.L., *The origin of the wind tunnel in Europe, 1871-1900*, in *Air Power History*. 1998, Air Force Historical Foundation: Rockville. p. 4-15.
2. Kliche, D., C. Mundt, and E.H. Hirschel, *The hypersonic Mach number independence principle in case of viscous flow.* Shock waves, 2011. **21**(4): p. 307-314.
3. Pope, A. and K.L. Goin, *High-Speed Wind Tunnel Testing*. 1978: Robert E. Krieger.
4. Eugene N. A. Hoffman, I.P.B., and Christopher S. Combs, *Construction of a Mach 7 Ludwieg Tube at UTSA.* AIAA AVIATION 2020 Forum, 2020.
5. Sandham, N.D., *Effects of Compressibility and Shock-Wave Interactions on Turbulent Shear Flows.* Flow, turbulence and combustion, 2016. **97**(1): p. 1-25.
6. Amos, S.W. and R.S. Amos, *Pitot, Henri (1695 - 1771)*. 1992, Elsevier Science and Technology.
7. Allaby, M., *pitot tube (pitot—static tube)*, in *Encylopedia of Weather and Climate*. 2002, Facts on File. p. 425-426.
8. Lindsay, G.A., *Pressure Energy and Bernoulli's Principle.* American Journal of Physics, 1952. **20**(2): p. 86-88.
9. Anderson, J., *Modern Compressible Flow: With Historical Perspective / Edition 3*. 3rd ed. 2002: McGraw-Hill Higher Education.
10. Abernathy, F.H., *Film Notes for Fundamentals of Boundary Layers*. 1970, Encyclopedia Britannica Educational Corporation: Education Development Center, Inc.
11. Grilli, M., et al., *Analysis of unsteady behaviour in shockwave turbulent boundary layer interaction.* Journal of Fluid Mechanics, 2012. **700**: p. 16-28.
12. Mayle, R.E., *The 1991 IGTI Scholar Lecture: The Role of Laminar-Turbulent Transition in Gas Turbine Engines.* Journal of turbomachinery, 1991. **113**(4): p. 509-536.
13. Délery, J. and J.-P. Dussauge, *Some physical aspects of shock wave/boundary layer interactions.* Shock waves, 2009. **19**(6): p. 453-468.
14. Bashor, I., et al., *Design and Preliminary Calibration of the UTSA Mach 7 Hypersonic Ludwieg Tube*, in *AIAA Aviation 2019 Forum*. 2019, American Institute of Aeronautics and Astronautics.

15. Hoffman, E.N., et al., *Preliminary Testing of the UTSA Mach 7 Ludwieg Tube*, in *AIAA Aviation 2021 Forum*. 2021, American Institute of Aeronautics and Astronautics, Inc. : Virtual.
16. Hoffman, E.N.A., et al., *Characterization of the UTSA Mach 7 Ludwieg Tube.* AIAA SciTech Forum, 2022.